Ban *et al. Appl Biol Chem* (2020) 63:63
https://doi.org/10.1186/s13765-020-00549-3

KSABC
The Korean Society for Applied Biological Chemistry

ARTICLE Open Access

Human neutrophil elastase inhibitory dihydrobenzoxanthones and alkylated flavones from the *Artocarpus elasticus* root barks

Yeong Jun Ban[1†], Aizhamal Baiseitova[1†], Mohd Azlan Nafiah[2], Jeong Yoon Kim[1] and Ki Hun Park[1*]

Abstract

Neutrophil elastases are deposited in azurophilic granules interspace of neutrophils and tightly associated with inflammatory ailments. The root barks of *Artocarpus elasticus* had a strong inhibitory potential against human neutrophil elastase (HNE). The responsible components for HNE inhibition were confirmed as alkylated flavones (**2**–**4**, $IC_{50} = 14.8 \sim 18.1$ μM) and dihydrobenzoxanthones (**5**–**8**, $IC_{50} = 9.8 \sim 28.7$ μM). Alkyl groups on flavone were found to be crucial functionalities for HNE inhibition. For instance, alkylated flavone **2** ($IC_{50} = 14.8$ μM) was 20-fold potent than mother compound norartocarpetin (**1**, $IC_{50} > 300$ μM). The kinetic analysis showed that alkylated flavones (**2**–**4**) were noncompetitive inhibition, while dihydrobenzoxanthones (**5**–**8**) were a mixed type I ($K_I < K_{IS}$) inhibitors, which usually binds with free enzyme better than to complex of enzyme–substrate. Inhibitors and HNE enzyme binding affinities were examined by fluorescence quenching effect. In the result, the binding affinity constants (K_{SV}) had a significant correlation with inhibitory potencies (IC_{50}).

Keywords: Alkylated flavones, *Artocarpus elasticus*, Dihydrobenzoxanthones, Fluorescence quenching, Human neutrophil elastase inhibition (HNE)

Introduction

Serine proteases are the largest and most important unit among the enzyme groups found in eukaryotes and prokaryotes, which distinctively increases the reaction of the peptide bonds hydrolysis [1]. One of them the neutrophil elastase (NE, EC 3.4.21.37) 29 kDa chymotripsis family protease, largely expressed by neutrophils precursors inside the bone marrow, then in its mature active form they placed in primary (azurophilic) granules [2]. Throughout inflammation spread into the cell interspace NE activity closely contained by an abundant blood plasma inhibitor—α1-antytrypsin (AAT) [3]. The stoppage of releasing AAT in hepatocytes expressively decreases its levels, leading to emphysema because of deficient defence of the lower respiratory tract from human neutrophil elastase (HNE), and further alveoli damage [4]. This leads to the development of the chronic obstructive pulmonary disease, emphysema and lung cancer, also in the liver, it causes benign neonatal hepatitis syndrome, fibrosis which evolves to cirrhosis and even to hepatocellular carcinoma [5]. Augmentation therapy has been accepted as the best therapy for AAT deficiency, and less costly methods such as low molecular weight NE inhibitors have failed clinically, despite diligent efforts over the past three decades [6]. On the other hand, the release of granular contents leads to the recruitment of inflammatory cells through cytokines (TNF-α, IL-1β, IL-6, IL-18, IL-10), adipokines (adiponectin, resistin and leptin), and chemokines (IL-8), which are the main intermediaries and progressors of renal tissue damage [7]. Thus, the invention of novel protease inhibitors is an invaluable therapeutic tool. There have been many attempts to develop lead structures for inhibiting HNE from plant sources [8, 9].

*Correspondence: khpark@gnu.ac.kr
†Yeong Jun Ban and Aizhamal Baiseitova contributed equally to this work
[1] Division of Applied Life Science (BK21 plus), IALS, Gyeongsang National University, Jinju 52828, Republic of Korea
Full list of author information is available at the end of the article

Artocarpus elasticus, which common name is Terap, from the Moraceae family, distributed in the Asian tropics. The plant is widely used in food: peeled shoot tips and fleshy perianth can even be eaten raw, and the seeds are eaten fried. The ripe fruits are edible, but they often have an unpleasant smell. Leaves were used for nursing mothers, young leaves to treat vomiting, diseases related to blood, the bark inner side was used to treat sores, and latex also used in dysentery, fever, hypertension and diabetes [10, 11]. The therapeutic effect is associated with the abundance of phenolics, such as flavonoids, stilbenoids, dihydrochalcones, dihydrobenzoxanthones and prenylated flavonoids [12]. Single metabolites reported in vivo antimalarial [13], inhibition of LPS-induced inflammation [14], α-glucosidase inhibitory [15], TRAIL-resistance overcoming with antiviral [16], and anticancer [17] activities. Alkylated flavonoid Artonin E from *A. elasticus* also revealed considerable cytotoxic effect in MCF-7 human breast cancer cells by ROS mediated mitochondrial pathway [18, 19]. In particular, metabolites in *A. elasticus* has not been reported to have HNE inhibitory potential capacity.

The aim of the present study was the investigation of HNE inhibitory potential of the root barks of *A. elasticus*, and to isolate the responsible components for HNE inhibition. The inhibitory mechanisms were fully characterized by double reciprocal plots from the Michaelis–Menten equation. We also tried to determine the binding affinities of the isolated inhibitors to HNE enzyme by fluorescence (FS) quenching experiment.

Materials and methods

Instruments and chemicals

Bruker AM500 spectrometer (Karlsruhe, Germany) used for measurement of proton and carbon-13 NMR spectra. By mass spectrometer JEOL JMS-700 (Tokyo, Japan) obtained all mass data. Forte/R 100 (YMC, Kyoto, Japan) recycling HPLC and MPLC with Triart C18 column (YMC, Japan) used for isolation of compounds. Methanol, acetonitrile, water and acetic acid of the analytical grade for HPLC were purchased from Fisher Scientific (Korea). For performing enzyme assays SpectraMax M3 Multi-Mode Microplate Reader (Molecular device, USA) was used. HNE (EC 3.4.21.37) was ordered from Sigma Aldrich (St. Louis, USA).

Plant material

Collection in December 2013 and storage until extraction of Malaysian the *A. elasticus* barks done by associated professor Dr. Mohd Azlan Nafiah. The voucher of the specimen (TM1016) was given in the Universiti Pendidikan Sultan Idris, Malaysia.

Extraction and isolation

Extraction of *A. elasticus* barks (250 g) was done in methanol (10L), at approximately 25 °C, resulting to crude reddish-brown colour gum (27 g). The methanol extract was dried well and dissolved in 500 mL of water to be suspended for further fractionation into dark-red chloroform extract (dry weight 14 g). Then chloroform extract was chromatographed by MCI GEL CHP20P (30 × 5 cm, 75–150 µm, 500 g) column with step by step changing of water/methanol system (8:2 → 0:1) resulting to A1-15 fractions. Nonpolar A8-12 fractions (total 4.6 g) were refractionated by MPLC (using ODS column 25 × 3 cm, S-10 µm, 12 nm, YMC) with a slow changing of solvents from water to MeOH (0 → 100%) to give B1-80 subfractions. The subfractions B26-35, totally 1.8 g, were further subjected to recycling HPLC (using ODS column 25 × 3 cm, S-5 µm, 12 nm, YMC), which resulted to the isolation of compounds **1** (38 mg), **3** (21 mg), and **8** (35 mg). Likewise, the subfractions B36-43 total 1.4 g, were put to recycling HPLC to isolate dihydrobenzoxanthone **5** (14 mg), **6** (22 mg), and alkylated flavone **4** (19 mg). In the same way, the subfractions B44-56 (1.5 g) were also recycled on HPLC to purify compounds **2** (12 mg) and **7** (18 mg). Purification of compounds done on Sephadex-LH20.

Measurement of HNE inhibitory activity

The inhibitory activity of HNE (EC 3.4.21.37) was analysed by measuring of the hydrolysis of *N*-methoxysuccinyl-Ala–Ala-Pro-Cal-*p*-nitroanilide at 405 nm in optimal pH of 8.0 (0.02 mM, Tris–HCl buffer) and at 37 °C [8]. In brief, to 96-well plates 10 µL the inhibitors or caffeic acid as a control (dissolved in DMSO), 40 µL substrate (MeOSuc-AAPV-*p*NA, 1.5 mM), 130 µL of buffer and 20 µL enzyme (stock concentration 0.2 unit/mL) mixed. The concentration of 50% inhibition of the enzyme (IC_{50}) was expressed as compounds activity. Inhibition rate (%) calculated by next Eq. (1):

$$\text{Activity (\%)} = [1 + ([I]/IC_{50})] \times 100 \quad (1)$$

HNE inhibitory kinetic assay

By the same way with activity experiments, the enzyme kinetic behaviours were identified using MeOSuc-AAPV-*p*NA substrate concentrations of 0, 0.75, 1.5, and 3 mM with different concentrations of inhibitors [8]. Data analysis on Sigma Plot (Chicago, USA) used to determine the variables of curves. By Lineweaver–Burk plots, kinetic values such as Michaelis–Menten (K_m) and maximum velocity (V_{max}) were determined. From Dixon plots, enzyme and inhibitors (K_i) dissociation constants calculated. Constants of inhibitions when compounds binding whether free enzyme or else enzyme–substrate complex,

were calculated from plots of the slopes of the straight lines (K_I) or vertical intercept (K_{IS}) verse the concentration of inhibitors by Eqs. (2)–(4).

$$1/V = K_m/V_{max}(1 + [I]/K_I)\ 1/S + 1/V_{max} \quad (2)$$

$$\text{Slope} = K_m/K_I V_{max}[I] + K_m/V_{max} \quad (3)$$

$$\text{Intercept} = 1/K_{IS} V_{max}[I] + K_m/V_{max}. \quad (4)$$

Measurement of binding affinity to the enzyme

In the 96-well black immuno-plates the reaction mixture of 180 µl of 0.02 mM Tris–HCl buffer (pH 8.0) with 10 µl of HNE (0.2 unit/mL) were added into the 10 µl inhibitors with concentrations of 0, 3.125, 6.25, 12.5, 25 and 50 µM [8]. FS quenching spectra were obtained using a spectrophotometer (SpectraMax M3) at the emission of from 300 to 400 nm (excitation 295 nm) with slits of 2.0 nm.

Statistical analysis

Experiments were repeated thrice, then analyzed on SigmaPlot (v. 10.0), $p < 0.05$ were determined as a noteworthy alteration.

Results and discussions

Isolation of HNE inhibitors from *A. elasticus* root barks

Artocarpus elasticus has been proven to possess anti-inflammatory activities that might be associated with HNE enzyme. In the primary experiment, the root barks methanol extract of target plant presented a significant potential (50 µg/mL, 80% inhibition) against HNE. This encourages us to examine HNE inhibitory metabolites from the root part of this species. The methanol extracts of the root barks were fractionated by solvents with different polarities (hexane, chloroform, ethyl acetate, water) for further isolation based on HNE inhibitory potencies. The chloroform fractions were purified by chromatography over octadecyl-functionalized silicagel and Sephadex LH-20 to yield eight compounds. As shown in Fig. 1, compounds were identified as norartocarpetin (**1**), artoflavone B (**2**), KB 2 (**3**), artonin E (**4**), artobiloxanthone (**5**), artoindonesianin W (**6**), cycloartobiloxanthone (**7**), and artoindonesianin P (**8**) by obtained spectra (see Additional file 1), with the comparison to the published data [20, 21].

Among the isolated compounds we elucidated the most active inhibitor dihydrobenzoxanthone **5** chemical structure. The compound **5** has a molecular formula $C_{25}H_{22}O_7$ as established by the $[M]^+$ ion at 434.1363 (Calcd for 434.1366) in HREIMS analysis. A five cyclic skeleton of this compound was deduced by extra 5 unsaturation degrees from calculation of double bonds. The D-ring was deduced by the unique of endomethylene $H9_{a/b}$ (δ_H 2.51 and 3.47) and propenyl functionality (δ_H 1.86, 4.07, 4.38, and 4.07). The presence of C10 propenyl moiety was obtained by HMBC correlation of H10 (δ_H 4.07) to C11 (δ_C 150.9). The pyran group was established from proton coupling of H14 (δ_H 6.99, d) to H15 (δ_H 5.73, d) and HMBC correlation between H14a and oxygenated carbon C15 (δ_C 129.88). The locations of methyls were deduced from HMBC of both H17 (δ_H 1.51) and H18 (δ_H 1.54) to C15. From this the compound **5** was identified as 8,9-dihydro-6,10,11,13-tetrahydroxy-3,3-dimethyl-9-(1-methylethenyl)-3H,7H-benzo[c]pyrano[3,2-h]xanthen-7-one and named as artobiloxanthone.

HNE inhibitory activity of isolated compounds and their kinetics

HNE inhibitory activities of the isolated flavones at different concentrations (**1**–**8**) screened using a UV assay according to a previously reported method [8, 22]. All isolates inhibited in a dose-dependent manner the HNE enzyme, but alkylated flavones (**2**–**4**) and dihydrobenzoxanthones (**5**–**8**) showed much higher inhibitions than mother skeleton, norartocarpetin (**1**), their IC_{50}s given in Table 1. As shown in Fig. 2a, both compounds **1** and **2** showed a discriminatory dose-dependence curve. The alkylated flavone **2** ($IC_{50} = 14.8$ µM) was 20-fold active than mother compound **1** ($IC_{50} > 300$ µM). The similar inhibitory tendency was also observed from other alkylated flavones **3** and **4**, which indicated that the prenyl group on C3 was a crucial functionality to HNE inhibition. Dihydrobenzoxanthones (**5**-**8**) inhibited HNE significantly with IC_{50} values of 9.8 ~ 28.7 µM, compared to the mother compound. The number of the hydroxyl group of B-ring affected inhibitory capacities as follow: compounds **5** ($IC_{50} = 9.8$ µM) versus **8** ($IC_{50} = 28.7$ µM).

Reversibility between inhibitor and HNE enzyme was confirmed by the plotting activity of residual enzyme inhibited with different concentrations of inhibitor versus the enzyme concentration. Inhibitors showed a comparable plotting tendency between enzyme activity and concentration as like in Fig. 2b. As shown in Fig. 2b, increasing of representative inhibitors **2** concentrations caused a reduction of the slopes of lines, of which the straight lines family was passed through the beginning of coordinates. This phenomenon indicated that inhibitor **2** had reversibility to the enzyme.

The characterization of the inhibitory mechanism was showed off using Michaelis–Menten double reciprocal plots. First of all alkylated flavones (**2**–**4**) were confirmed as noncompetitive inhibitors, because of no change of K_m and the decrease of V_{max} as shown in Figs. 2c and 3a insets. Figures 2c and 3a elucidated Lineweaver–Burk

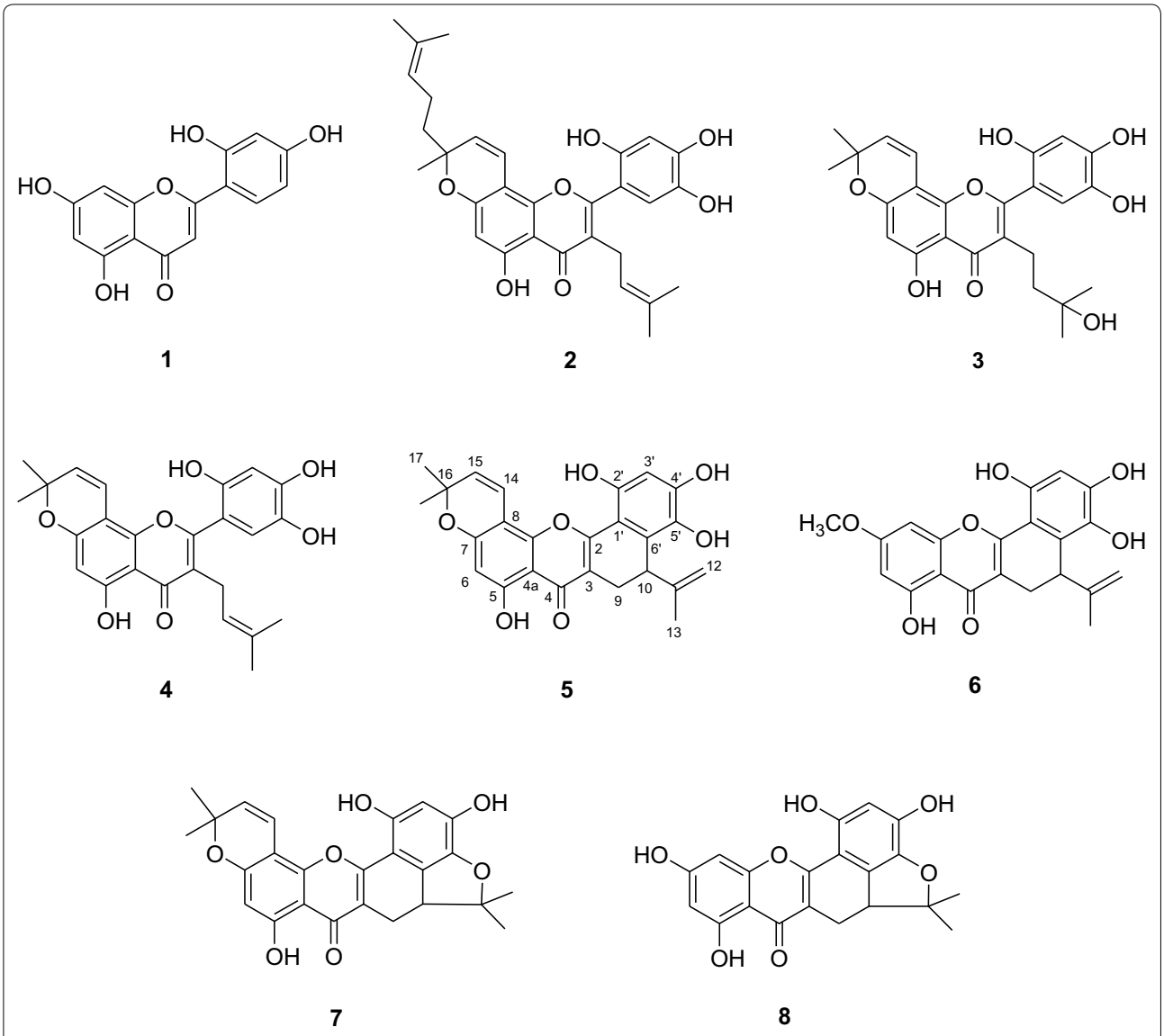

Fig. 1 The chemical structures of compounds **1**–**8** isolated from the root barks of *A. elasticus*

plots of alkylated flavones **2** and **3**, which have a common intercept on the x-axis at different inhibitor concentrations. The K_i values of **2** and **3** was calculated to be 12.6 μM and 15.4 μM, respectively by Dixon plots (Figs. 2d and 3b and Table 1). In the case of dihydrobenzoxanthones (**5**-**8**), they were determined as mixed type inhibitors. Since increasing of the inhibitor concentrations resulted in a common intercept of the family of lines on the left of the y-axis and above the x-axis as like Fig. 3c and e. The mixed type inhibitors usually have a dissimilar affinity to the substrate (mixed type I) and to the free enzyme (mixed type II). The results of the measured velocity of compounds **5** and **6** were fitted to the Eqs. (3) and (4) for the calculation of K_I and K_{IS} by secondary plots of K_m/V_{max} and $1/V_{max}$ *versus* compound concentrations. In particular, compound **5** was found to be mixed type I ($K_I = 6.5$ μM $< K_{IS} = 31.8$ μM), as like compound **6** ($K_I = 4.7$ μM $< K_{IS} = 19.9$ μM). At last, the K_i values of compounds **5** and **6** were determined to be 6.4 and 4.7 μM respectively, by Dixon plots (Fig. 3d and f, Table 1).

Binding affinities between HNE and compounds

Intrinsic fluorescence (FS) intensity of protein usually changes as a function of ligand concentration when protein acts together with another ligands [23]. Generally,

Table 1 Inhibitory effects of compounds on HNE

Compounds	IC_{50}^{a} (μM)	Inhibition mode (K_i^b, μM)	K_I (μM)	K_{IS} (μM)
1	> 300	NT	NT	NT
2	14.8 ± 0.4	Noncompetitive (12.6 ± 0.2)	NT	NT
3	16.0 ± 0.4	Noncompetitive (15.4 ± 0.4)	NT	NT
4	18.1 ± 0.3	Noncompetitive (17.7 ± 0.6)	NT	NT
5	9.8 ± 0.1	Mixed (6.4 ± 0.5)	6.5	31.8
6	11.2 ± 0.1	Mixed (4.7 ± 0.5)	4.7	19.9
7	20.8 ± 0.3	Mixed (13.7 ± 0.2)	13.8	46.9
8	28.7 ± 0.7	Mixed (19.4 ± 0.3)	17.5	31.2
Caffeic acid[c]	67.1 ± 0.2	NT	NT	NT

NT not tested

[a] Sample concentration which led to 50% enzyme activity loss

[b] K_i is the inhibition constant

[c] The positive control

intrinsic FS of protein originates from phenylalanine (Phe), tryptophan (Trp) and tyrosine (Tyr) residues. The most sensitive fluorophore residue is a Trp [24]. HNE enzyme has a suitable FS intensity due to three residues of Trp (Trp-12, Trp-127, and Trp-212) [25]. The binding affinity of compounds with HNE was determined by FS quenching effects. There is no measurable emission from other ingredients of the mixture solution in the current experiment conditions (em. 300 ~ 400 nm). Figure 4 showed the effects of FS quenching of the representative compounds **1**, **2** and **8** at the same concentrations (0 → 50 μM). FS intensity was decreased by inhibitor concentrations, but quenching affinities allowed to their HNE inhibitory activities. As shown in Fig. 4c, one of the most active compound **2** (IC_{50} = 14.8 μM) quenched FS intensity dose-dependently, to be almost complete quenched at 50 μM concentration. FS quenching effect was not observed from mother compound **1**

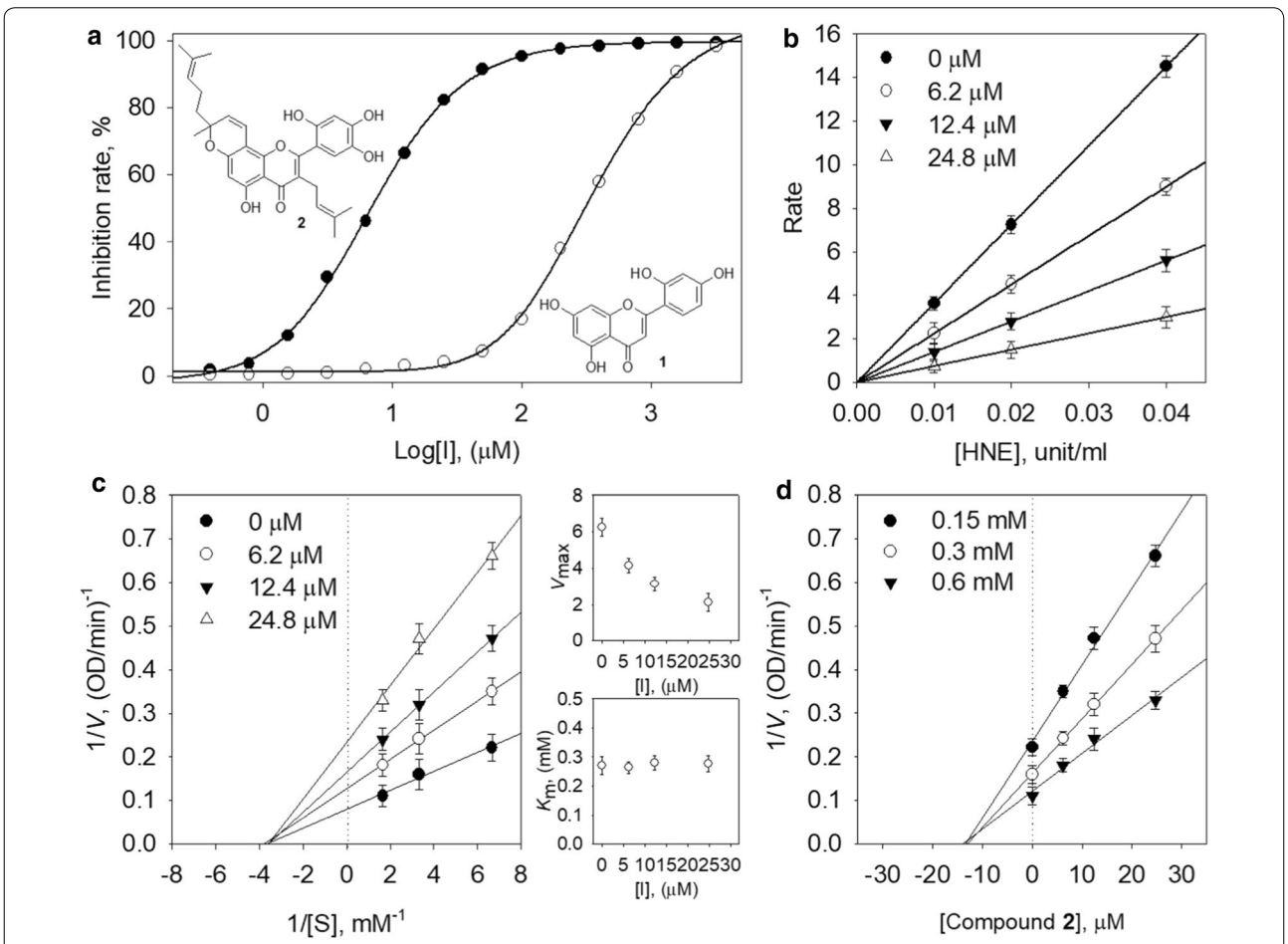

Fig. 2 Enzyme inhibition activity of compounds **1** and **2** against human neutrophil elastase (HNE). **a** Dose-dependent effect of the compounds **1** and **2** on HNE. **b** The catalytic activity of HNE as a function of enzyme concentration at different concentrations of compound **2**. **c** Lineweaver–Burk plots of compound **2**. (Inset) Tendencies for the maximal velocity (V_{max}) and Michaelis–Menten constants (K_m) for compound **2**. **d** Dixon plots of compound **2**

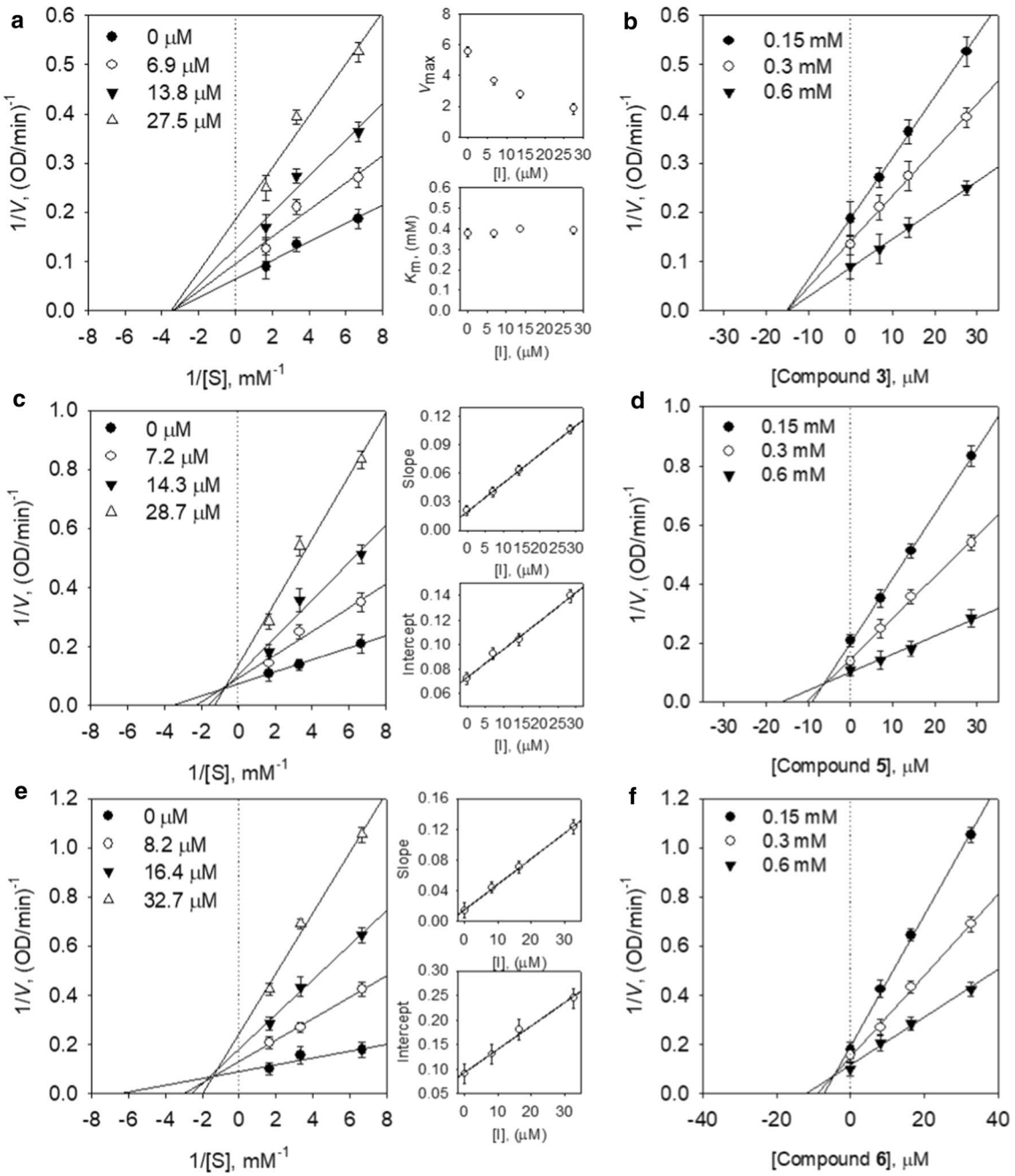

Fig. 3 Enzymatic kinetics of compounds **3**, **5**, and **6**. Lineweaver–Burk plots for HNE inhibition of **a** compounds **3**, **c** compound **5**, and **e** compound **6**. (Inset) **a** Tendencies for the maximal velocity (V_{max}) and Michaelis–Menten constants (K_m) for compound **3** and The secondary plots of the straight lines of slope and intercept *versus* the concentration of **c** compound **5** and **e** compound **6**. Dixon plots of **b** compounds **3**, **d** compound **5**, and **f** compound **6**

($IC_{50} > 300$ μM) at 50 μM concentration. The moderate compound **8** showed the average FS quenching effect also correlated with its inhibitory potency ($IC_{50} = 28.7$ μM). The parameters regarding binding affinity can be calculated by the following Eqs. (5)–(6):

$$F_0 - F = 1 + K_{SV}[Q_f] \tag{5}$$

$$\log\left[(F_0 - F)/F\right] = \log K_A + n \log[Q_f] \tag{6}$$

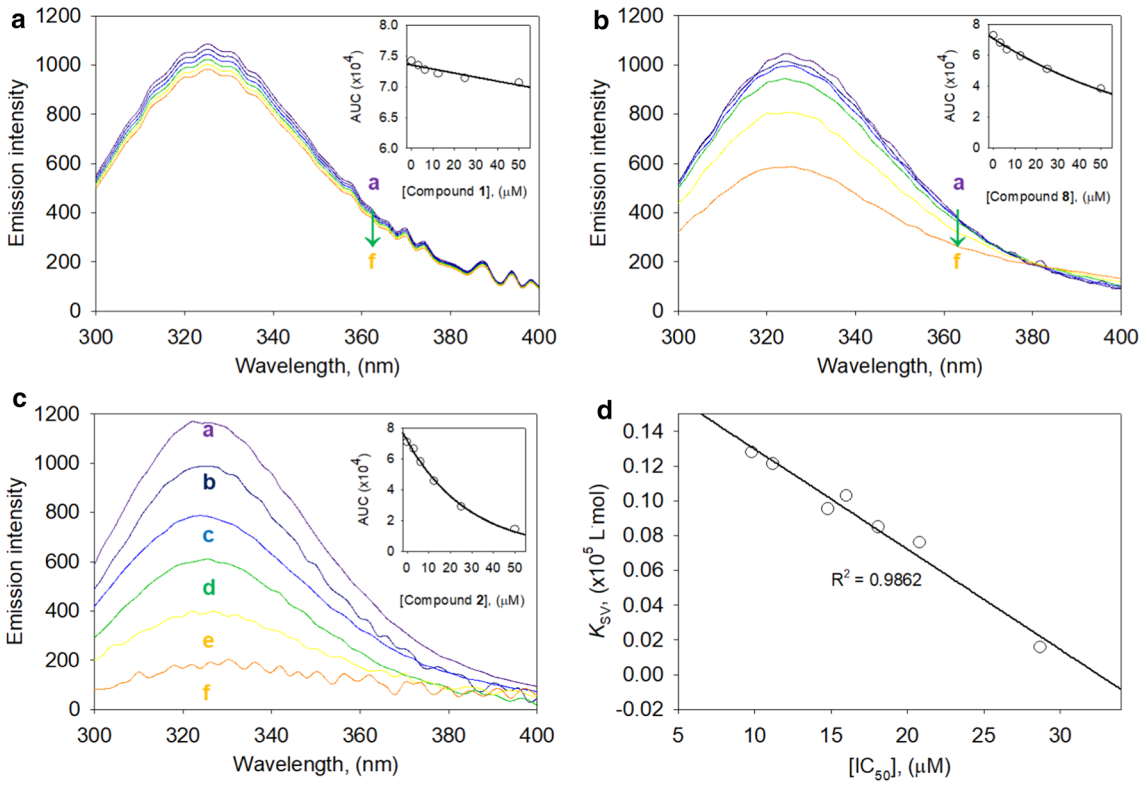

Fig. 4 The fluorescence spectra **a**-**c** of α-glucosidase at different concentrations (0, 3.125, 6.25, 12.5, 25.0, and 50.0 μM for curves a → f, $T = 37$ °C, **a** For compound **1**, **b** For compound **8**, **c** For compound **2**. (Inset) Areas under curves of fluorescence emission spectra for HNE are shown for compounds **1**, **8**, and **2**, respectively. **d** The correlation curve between the inhibitory potencies (IC_{50}s) and the Stern–Volmer constant (K_{SV})

Table 2 Fluorescence quenching effect of compounds 1–8 on HNE

Compounds	K_{SV} ($\times 10^5$ L mol^{-1})	R[a]	*n*	K_A ($\times 10^6$ L mol^{-1})	R[b]
2	0.0954	0.9896	1.1616	0.0486	0.9989
3	0.1029	0.9549	1.3636	0.0219	0.9938
4	0.0849	0.9793	1.1279	0.0330	0.9830
5	0.1280	0.9722	1.4117	0.0241	0.9985
6	0.1212	0.9766	1.3934	0.0252	0.9993
7	0.0760	0.9965	1.2574	0.0510	0.9978
8	0.0158	0.9800	1.1955	0.0064	0.9851

[a] R is the correlation coefficient for the K_{SV} values

[b] R is the correlation coefficient for the K_A values

F_0 and F were the FS emission intensities in the absence or presence of a quencher, respectively. [Q_f] is a concentration of compounds, n is a binding sites number, and K_A is a binding constant. Binding parameters (K_{SV}, K_A, and n) of the compounds were calculated. Stern–Volmer constants (K_{SV}) shown in Table 2 had a significant correlation with their inhibitory potencies (IC_{50}). For example, compound **2** ($IC_{50} = 14.8$ μM, $K_{SV} = 0.0954 \times 10^5$ L mol^{-1}) had 6-fold higher value of K_{SV} than 8 ($IC_{50} = 28.7$ μM, $K_{SV} = 0.0158 \times 10^5$ L mol^{-1}). As well, all compounds Stern–Volmer constants strongly correlated ($R^2 = 0.9862$) to IC_{50}. These results designate a single binding site of inhibitors to HNE enzyme.

Supplementary information

Supplementary information accompanies this paper at https://doi.org/10.1186/s13765-020-00549-3.

Additional file 1. Supplementary information includes NMR spectroscopic data of compounds, **Figs. S1–S26.** 1D, 2D NMR, and HRMS data of compounds **1**–**8**, **Fig. S27.** Enzyme kinetic data of compounds **4**, **7**, and **8**. **Fig. S28.** The fluorescence effect of compounds **3**–**7**.

Acknowledgements
Not applicable.

Authors' contributions
AB and JYK screened HNE inhibitory activity of isolated compounds. YJB and AB isolated and identified compounds from *A. elasticus*. MAN provided plant material *A. elasticus* and make suggestions about overall research. KHP designed overall research. All authors read and approved the final manuscript.

Funding
This work was done with research funds from the Ministry Education, Republic of Korea through the National Research Foundation (NRF) grant funded by the South Korea government (2018R1A2B6001753) and the Next-Generation BioGreen 21 program, Rural Development Administration (SSAC, No. PJ01318601), Republic of Korea. The BK21 Plus program supported scholarships for all students.

Availability of data and materials
All data analysed throughout this study are available in this published article and its Additional file 1.

Competing interests
Authors declare no conflict interests.

Author details
[1] Division of Applied Life Science (BK21 plus), IALS, Gyeongsang National University, Jinju 52828, Republic of Korea. [2] Department of Chemistry, Faculty of Science and Mathematics, Universiti Pendidikan Sultan Idris, 35900 Tg. Malim, Perak, Malaysia.

Received: 26 August 2020 Accepted: 15 September 2020
Published online: 29 September 2020

References

1. António JPM, Gonçalves LM, Guedes RC, Moreira R, Gois PMP (2018) Diazaborines as new inhibitors of human neutrophil elastase. ACS Omega 3(7):7418–7423. https://doi.org/10.1021/acsomega.8b00702
2. Jugniot N, Voisin P, Bentaher A, Mellet P (2019) Neutrophil elastase activity imaging: recent approaches in the design and applications of activity-based probes and substrate-based probes. Contrast Media Mol Imaging 2019:1–12. https://doi.org/10.1155/2019/7417192
3. Dau T, Sarker RSJ, Yildirim AO, Eickelberg O, Jenne DE (2015) Autoprocessing of neutrophil elastase near its active site reduces the efficiency of natural and synthetic elastase inhibitors. Nat Commun 6(1):6722. https://doi.org/10.1038/ncomms7722
4. Siedle B, Hrenn A, Merfort I (2007) Natural compounds as inhibitors of human neutrophil elastase. Planta Med 73(5):401–420. https://doi.org/10.1055/s-2007-967183
5. Alasbahi R (2008) The in vitro inhibition of human neutrophil elastase activity by some Yemeni medicinal plants. Sci Pharm 76(3):471–484. https://doi.org/10.3797/scipharm.0804-25
6. Polverino E, Rosales-Mayor E, Dale GE, Dembowsky K, Torres A (2017) The role of neutrophil elastase inhibitors in lung diseases. Chest 152(2):249–262. https://doi.org/10.1016/j.chest.2017.03.056
7. Bronze-da-Rocha E, Santos-Silva A (2018) Neutrophil elastase inhibitors and chronic kidney disease. Int J Biol Sci 14(10):1343–1360. https://doi.org/10.7150/ijbs.26111
8. Kim JY, Wang Y, Uddin Z, Song YH, Li ZP, Jenis J, Park KH (2018) Competitive neutrophil elastase inhibitory isoflavones from the roots of Flemingia philippinensis. Bioorg Chem 78:249–257. https://doi.org/10.1016/j.bioorg.2018.03.024
9. Tan XF, Kim DW, Song YH, Kim JY, Yuk HJ, Wang Y, Curtis-Long MJ, Park KH (2016) Human neutrophil elastase inhibitory potential of flavonoids from Campylotropis hirtella and their kinetics. J Enzyme Inhib Med Chem 31(sup1):16–22. https://doi.org/10.3109/14756366.2015.1118683
10. Jagtap UB, Bapat VA (2010) Artocarpus: a review of its traditional uses, phytochemistry and pharmacology. J Ethnopharmacol 129:142–166. https://doi.org/10.1016/j.jep.2010.03.031
11. Lim TK (2012) Edible Medicinal And Non Medicinal Plants. Springer, Netherlands, Dordrecht. https://doi.org/10.1007/978-94-007-2534-8
12. Hakim A (2010) Diversity of secondary metabolites from Genus Artocarpus (Moraceae). Nusant Biosci 2(3):146–156. https://doi.org/10.13057/nusbiosci/n020307
13. Suhartati T, Epriyanti E, Yandri Borisha I, Suwandi JF, Quwono SD, Qudus HI, Hadi S (2020) In vivo antimalarial test of artocarpin and in vitro antimalarial test of Artonin M isolated from Artocarpus. Rev Chim 71(5):400–408. https://doi.org/10.37358/RC.20.5.8150
14. Hankittichai P, Buacheen P, Pitchakarn P, Takuathung MN, Wikan N, Smith DR, Potikanond S, Nimlamool W (2020) *Artocarpus lakoocha* extract inhibits LPS-induced inflammatory response in RAW 264.7 Macrophage Cells. Int J Mol Sci 21(4):1355. https://doi.org/10.3390/ijms21041355
15. Jenis J, Baiseitova A, Yoon SH, Park C, Kim JY, Li ZP, Lee KW, Park KH (2019) Competitive α-glucosidase inhibitors, dihydrobenzoxanthones, from the barks of *Artocarpus elasticus*. J Enzyme Inhib Med Chem 34(1):1623–1632. https://doi.org/10.1080/14756366.2019.1660653
16. Toume K, Habu T, Arai MA, Koyano T, Kowithayakorn T, Ishibashi M (2015) Prenylated flavonoids and resveratrol derivatives isolated from *Artocarpus communis* with the ability to overcome TRAIL resistance. J Nat Prod 78(1):103–110. https://doi.org/10.1021/np500734t
17. Pedro M, Ferreira MM, Cidade H, Kijjoa A, Bronze-da-Rocha E, Nascimento MSJ (2005) Artelastin is a cytotoxic prenylated flavone that disturbs microtubules and interferes with DNA replication in MCF-7 human breast cancer cells. Life Sci 77(3):293–311. https://doi.org/10.1016/j.lfs.2004.09.049
18. Etti IC, Abdullah R, Kadir A, Mohd Hashim N, Yeap SK, Imam MU, Ramli F, Malami Lam KL, Etti U, Waziri P, Rahman M (2017) The molecular mechanism of the anticancer effect of Artonin E in MDA-MB 231 triple negative breast cancer cells. PLoS ONE 12(8):e0182357. https://doi.org/10.1371/journal.pone.0182357
19. Etti IC, Rasedee A, Mohd Hashim N, Abdul AB, Kadir A, Yeap SK, Waziri P, Malami I, Lim KL, Etti CJ (2017) Artonin E induces p53-independent G1 cell cycle arrest and apoptosis through ROS-mediated mitochondrial pathway and livin suppression in MCF-7 cells. Drug Des Devel Ther 11:865–879. https://doi.org/10.2147/DDDT.S124324
20. Jayasinghe ULB, Samarakoon TB, Kumarihamy BMM, Hara N, Fujimoto Y (2008) Four new prenylated flavonoids and xanthones from the root bark of *Artocarpus nobilis*. Fitoterapia 79(1):37–41. https://doi.org/10.1016/j.fitote.2007.07.014
21. Hakim EH, Asnizar Yurnawilis, Aimi N, Kitajima M, Takayama H (2002) Artoindonesianin P, a new prenylated flavone with cytotoxic activity from Artocarpus lanceifolius. Fitoterapia 73(7–8):668–673. https://doi.org/10.1016/S0367-326X(02)00226-5
22. Kim JY, Lee JH, Song YH, Jeong WM, Tan X, Uddin Z, Park KH (2015) Human Neutrophil Elastase Inhibitory Alkaloids from *Chelidonium majus* L. J Appl Biol Chem 58(3):281–285. https://doi.org/10.3839/jabc.2015.044
23. Papadopoulou A, Green RJ, Frazier RA (2005) Interaction of flavonoids with bovine serum albumin: a fluorescence quenching study. J Agric Food Chem 53(1):158–163. https://doi.org/10.1021/jf048693g
24. Burstein EA, Vedenkina NS, Ivkova MN (1973) Fluorescence and the location of tryptophan residues in protein molecules. Photochem Photobiol 18(4):263–279. https://doi.org/10.1111/j.1751-1097.1973.tb06422.x
25. Sinha S, Watorek W, Karr S, Giles J, Bode W, Travis J (1987) Primary structure of human neutrophil elastase. Proc Natl Acad Sci USA 84(8):2228–2232. https://doi.org/10.1073/pnas.84.8.2228

Publisher's Note